J Physiol Sci (2013) 63:299–310
DOI 10.1007/s12576-013-0268-5

ORIGINAL PAPER

Radial stability of the actomyosin filament lattice in isolated skeletal myofibrils studied using atomic force microscopy

Daisuke Miyashiro · Jun'ichi Wakayama · Nao Akiyama · Yuki Kunioka · Takenori Yamada

Received: 20 December 2012 / Accepted: 30 April 2013 / Published online: 21 May 2013

Abstract The radial stability of the actomyosin filament lattice in skeletal myofibrils was examined by using atomic force microscopy. The diameter and the radial stiffness of the A-band region were examined based on force–distance curves obtained for single myofibrils adsorbed onto cover slips and compressed with the tip of a cantilever and with the Dextran treatment. The results obtained indicated that the A-band is composed of a couple of stiffness components having a rigid core-like component. It was further clarified that these radial components changed the thickness as well as the stiffness depending on the physiological condition of myofibrils. Notably, by decreasing the ionic strength, the diameter of the A-band region became greatly shrunken, but the rigid core-like component thickened, indicating that the electrostatic force distinctly affects the radial structure of actomyosin filament components. The results obtained were analyzed based on the elementary structures of the filament lattice composed of cross-bridges, thin filaments and thick filament backbones. It was clarified that the actomyosin filament lattice is radially deformable greatly and that (1), under mild compression, the filament lattice is stabilized primarily by the interactions of myosin heads with thin filaments and thick filament backbones, and (2), under severe compression, the electrostatic repulsive interactions between thin filaments and thick filament backbones became predominant.

Keywords Skeletal myofibril · Actomyosin filament · Lattice stability · Electrostatic force · Atomic force microscopy

Abbreviations

AFM	Atomic force microscopy
AMPPNP	Adenyl-5′-yl-imidodiphosphate
EGTA	Ethylene glycol tetraacetic acid
PIPES	Piperazine-1,4-bis(2-ethanesulfonic acid)

Introduction

The structure of skeletal muscle fiber has been extensively studied in relation to the molecular basis for force production [1]. In the A-band region of muscle fiber, actin and myosin filaments overlap each other producing a regular double-hexagonal lattice, called the overlap region, where the contractile force is produced by the interaction of the myosin heads with thin filaments [2]. The contractility of muscle fiber depends on the extent of the filament overlap [3] and is impaired by radial compression [4, 5]. Thus, the axial as well as the radial structural stabilities of the actomyosin filament lattice are essential for the stable force production of muscle fiber.

The axial stability of the actomyosin filament lattice has been examined in relation to the shortening of muscle fiber [2], while its radial stability has been studied in connection with the molecular mechanism for the filamentous packing

D. Miyashiro · N. Akiyama · T. Yamada (✉)
Department of Physics (Biophysics Section), Tokyo University of Science, Tokyo, Japan
e-mail: yamada@rs.kagu.tus.ac.jp

J. Wakayama
Nanobiotechnology Laboratory (Food Engineering Division), National Food Research Institute, National Agriculture and Food Research Organization, Ibaraki, Japan

Y. Kunioka
Japan Science and Technology Agency, Innovation Plaza Ishikawa, Ishikawa, Japan

of tobacco mosaic virus [6–8]. It has been established for the tobacco mosaic virus that the molecules are packed with each other by the balance between the van der Waals attractive force and the electrostatic repulsive force [9]. However, the molecular mechanism for the lattice formation of actomyosin filament system is not yet fully established because of the myosin heads extruded from thick filaments and interacting with thin filaments [10].

So far, the radial stability of the actomyosin filament lattice has been examined for skeletal muscle fibers based on the spacing changes of the filament lattice by using the X-ray diffraction technique [11–13]. The recent technology of atomic force microscopy (AFM) has enabled us to study the surface structure and radial stiffness of myofibrils isolated from muscle fibers [14–16]. Extensive studies of myofibrils isolated from skeletal muscle fiber has clarified that their contractility is essentially the same as that of muscle fibers under various physiological conditions [17–21]. In the present study, therefore, we examined the radial stability of the actomyosin filament lattice in isolated single skeletal myofibrils by applying AFM technology.

Materials and methods

Preparation of myofibrils

Psoas muscles dissected from white rabbits were used for experiments. The care of animals and the experimental protocol were approved by the Animal Care and Use Committee of Tokyo University of Science. Myofibrils were prepared by mechanical homogenization of glycerinated skinned fibers of the psoas muscle, as previously described [14, 20]. Myofibrils were prepared fresh before each experiment.

AFM measurements

AFM measurements were made as previously described with an AFM instrument incorporated in an inverted optical microscope (NV2500; Olympus Optics, Tokyo, Japan) [14]. The experimental chamber for AFM experiments was a trough cut in a silicone rubber sheet and glued onto the surface of a glass cover slip (Matsunami, Osaka, Japan). After myofibrils were adsorbed onto the surface of the bottom cover slip, the experimental chamber was filled with a bathing solution and installed on the microscope stage of the AFM system. The physiological condition of the myofibrils was changed by changing the bathing solution.

Cantilevers were purchased from Olympus Optics: a soft type (OMCL-TR400PSA, spring constant of 20 pN/nm) and a hard type (OMCL-TR800PSA, spring constant of 50 pN/nm). Modified cantilevers were prepared by gluing either a glass bead (2 or 5 μm in diameter; Thermo Fisher Scientific, MA, USA) or a glass rod (1 μm in diameter and about 10 μm in length) to the tip of a commercial cantilever as previously described [16]. Soft-type cantilevers with a bead-tip (with 2-μm bead) were used if not otherwise stated.

Diameter and radial stiffness measurements of single myofibrils

The diameter and the radial stiffness of single myofibril were examined based on force–distance curves obtained by AFM measurements. Force–distance curves were obtained by approaching the cantilever to single myofibril preparations adsorbed onto the surface of cover slip at a velocity of 0.1 μm/s as shown in the left panel of Fig. 1a. When the tip of the cantilever hit the preparation, the cantilever deflects upwards, making the preparation indented as shown in the right panel of Fig. 1a. Based on the deflection of the cantilever, detected electro-optically, the force applied to the cantilever, the indentation of the preparation, and the force–distance curve, i.e., the force applied to cantilever as a function of the position of the cantilever, were obtained [14].

The diameter of single myofibrils, which are nearly cylindrical [2], is determined as the top height of a single myofibril preparation from the surface of the cover slip based on the positions of the cantilever. The radial stiffness of a single myofibril, the stiffness perpendicular to the fiber axis, changes in a complicated manner depending on how much the preparation is compressed. In the following,

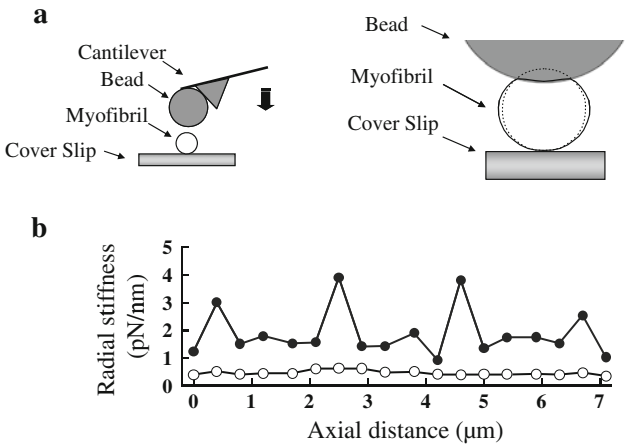

Fig. 1 **a** Schematics of (*left panel*) the AFM method of compressing a single myofibril adsorbed onto the surface of cover slip with the bead-tip of a cantilever and (*right panel*) the cross-section of the single myofibril compressed by the bead. **b** Radial stiffness distributions along a single myofibril in (*filled circle*) rigor and (*opened circle*) relaxed states

therefore, we analyzed the radial stiffness of single myofibrils determined as the force applied to the cantilever to make the surface of the preparation become indented by 0.1 μm, about 10 % of the diameter, if not otherwise stated. The diameter and radial stiffness of single myofibrils in various states were determined relative to those obtained for fresh myofibril preparations in a rigor state.

Axial stiffness measurements of single myofibrils

The axial stiffness of single myofibrils, the stiffness along the fiber axis, was determined based on the sinusoidal-length-change stiffness analysis for a single myofibril suspended between rigid and flexible glass needles in a separate experimental chamber filled with a bathing solution as detailed previously [20]. Sinusoidal length changes (0.5 % of the length of myofibril at 500 Hz) were applied to one end of the preparation via the rigid needle (elastic coefficient of about 10 N/m), and the force response detected at the other end based on the deflection of the flexible needle (elastic coefficient of about 0.5 N/m). The axial stiffness of the myofibril was determined as its force response over the sinusoidal length change applied. The physiological condition of the myofibrils was changed by changing the bathing solution appropriately.

Estimation of the radial and axial Young's moduli of myofibrils

The radial Young's modulus (E_R) of the A-band region of the myofibrils was determined for the indentation of single myofibrils slightly compressed with the rod-tip cantilever based on a regression analysis as previously described [14], by employing the Hertz equation for the indentation (δ) of an elastic rod produced by pressing a rigid rod in a criss-cross fashion [22] as,

$$\delta = \lambda \sqrt[3]{\frac{(R_1 + R_2)P^2}{2R_1R_2}\left(\frac{1-\sigma^2}{E_R}\right)^2}$$

where σ is the Poisson's ratio; λ, the Lame's constant; R_1, the radius of single myofibril; R_2, the radius of the rod at the tip of cantilever; and P, the force applied to cantilever. E_R was obtained by fitting the above equation to force–indentation curves which were transformed from force–distance curves obtained for the A-band region of single myofibrils. It was assumed that $\sigma = 0.5$, $\lambda = 2.1$, $R_1 = 0.5$ μm (based on the diameter of the single myofibril preparations determined below), and $R_2 = 0.5$ μm.

The axial Young's modulus of a single myofibril (E_A) was determined based on the sinusoidal-length-change stiffness analysis as,

$$E_A = \left(\frac{\Delta P}{\pi R^2}\right) \Big/ \left(\frac{\Delta L}{L_0}\right) = \left(\frac{L_0}{\pi R^2}\right)\left(\frac{\Delta P}{\Delta L}\right)$$

where L_0 is the length of myofibril; R, the radius of myofibril; ΔL, the amplitude of sinusoidal length change applied to myofibril; and ΔP, the amplitude of force response of myofibril. It was assumed that $\Delta L/L_0 = 0.005$ and $R = 0.5$ μm.

Composition of solutions

The composition of solutions was as follows (in mM); relaxing solution: K^+-propionate, 133; $MgCl_2$, 5; ethylene glycol tetraacetic acid (EGTA), 10; piperazine-1,4-bis(2-ethanesulfonic acid) (PIPES), 20; ATP, 5; rigor solution: K^+-propionate, 148; $MgCl_2$, 5; EGTA, 10; PIPES, 20; contracting solution: K^+-propionate, 155; $MgCl_2$, 5; $CaCl_2$, 2.3; EGTA, 2; PIPES, 20, ATP, 5; adenyl-5′-yl-diphosphate (AMPPNP) solution: K^+-propionate, 155; $MgCl_2$, 5; $CaCl_2$, 2.3; EGTA, 2; PIPES, 20; AMPPNP, 2.5. Solutions containing Dextran were prepared by dissolving appropriate amounts of Dextran T-500 and adjusting the composition of solutions appropriately. Solutions having various ionic strengths were prepared by adding appropriate amounts of KCl to solutions containing $MgCl_2$, 3; EGTA, 1; PIPES, 10; either ATP, 1 (for relaxing solutions) or ATP, 0 (for rigor solutions). The ionic strength of the bathing solutions was 200 mM if not otherwise stated. The free Ca concentrations for relaxing and contracting solutions were pCa = 9.0 and 4.0, respectively. The pH of all solutions was adjusted to 7.0. The ionic strength and the free Ca concentration of solutions were calculated as previously described [20].

ATP and AMPPNP were purchased from Sigma-Aldrich (MO, USA), and Dextran T-500 from GE Healthcare (Bucks, UK). All other chemicals were of analytical grade and purchased from Wako Chemicals (Osaka, Japan). All experiments were performed at room temperature (20–24 °C).

Statistics and curve fittings

Data values are expressed as the mean ± standard error of the mean with n = the number of myofibril preparations examined. Statistical significance tests were made by employing the paired and unpaired Student's t test appropriately. Regression analyses were made using IGOR Pro (v.3.14: WaveMetrics, OR, USA).

Results

Force–distance curve measurements for single myofibrils in various physiological conditions

First, A-band regions of single myofibrils adsorbed onto a cover slip were located, as previously described, based on

the radial stiffness distribution along myofibrils which was determined from force–distance curve measurements [14]. Typical stiffness distributions along single myofibrils in rigor and relaxing states are shown in Fig. 1b. A-band regions could readily be located for myofibrils in a rigor state inbetween rigid Z-bands running at an interval of about 2.1 μm [14, 23].

Typical force–distance curves obtained for A-band regions of single myofibrils in various physiological states are shown in Fig. 2a. The diameter of the A-band region of single myofibrils was 0.91 ± 0.10 μm ($n = 15$) in the rigor state, 0.92 ± 0.06 μm ($n = 15$) in the contracting state, 0.93 ± 0.04 μm ($n = 15$) in the (+)AMPPNP state, and 1.01 ± 0.04 μm ($n = 15$) in the relaxed state. Myofibrils were isometric in the contracting state as they were adsorbed onto the surface of the cover slip. The diameter of the A-band region in relaxed single myofibrils was significantly greater than that in other states ($p < 0.05$). It can be seen that the radial stiffness of myofibrils increases in the order of relaxed < (+)AMPPNP < contracting < rigor states, in agreement with the results of our previous AFM studies of skeletal myofibrils [14].

It can also be seen that each force–distance curve gets increasingly steep as the A-band regions are compressed by the cantilever, distinctly depending on the physiological condition of the myofibril. Further rigid core-like components, called the rigid core, could be seen in all force–distance curves examined, the thickness of which also changed depending on the physiological condition of the myofibril. The thickness of the rigid core was tentatively determined as the thickness of the A-band region compressed by the cantilever with a force of 4.0 nN, and its radial stiffness based on the slope of the force–distance curve there. The thickness of the rigid core thus determined was 0.57 ± 0.05 μm ($n = 5$) in rigor state and 0.43 ± 0.03 μm ($n = 5$) in relaxed state, slightly thicker in rigor state ($p < 0.05$), and their radial stiffnesses were approximately 10 pN/nm.

By being compressed by the tip of the cantilever, internal structures as well as their configurations of the A-band region would reversibly and irreversibly change depending on the extent of compression and the physiological condition of the myofibril [24]. To examine how the A-band region might be damaged by cantilever compressions, force–distance curve measurements were repeated at the same loci of the A-band region. In Fig. 2b are shown typical force–distance curves obtained for fresh rigor and relaxed myofibrils by using a hard-type cantilever, in which the first and second traces almost overlap each other. Consecutive traces similarly obtained almost overlap each other, suggesting that the A-band region could be reversibly compressed up to nearly 60 % of the diameter. In the following analysis, however, the first force–distance curves obtained at fresh A-band regions were used for analysis as in our previous studies [14].

Force–distance curve measurements for the A-band region of single myofibrils treated with Dextran

The force–distance curves of the A-band region examined above provide only qualitative characteristics of the internal structures of actomyosin filament lattice, as rod-shaped myofibril preparations were complicatedly compressed by a spherical tip of the cantilever as shown in the right panel

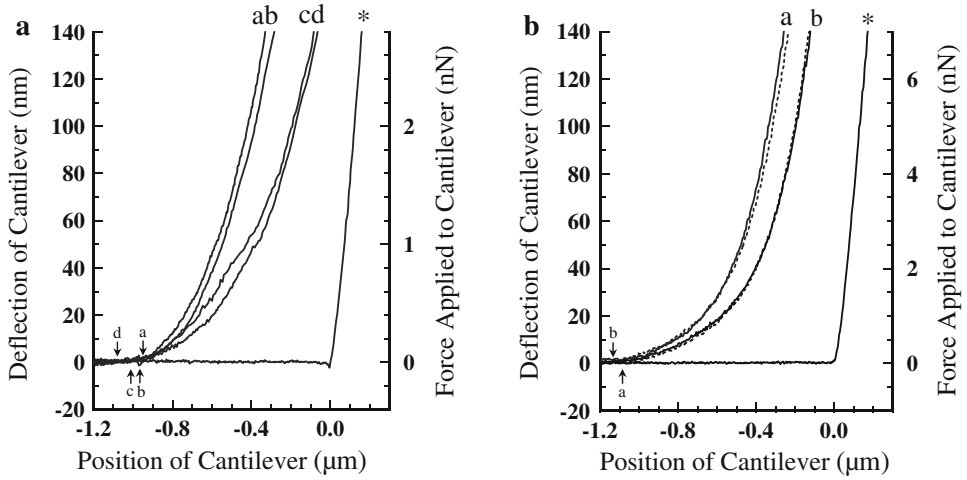

Fig. 2 **a** Force–distance curves obtained by using a soft-type cantilever for the A-band regions of single myofibrils in *a* rigor, *b* contracting, *c* (+)AMPPNP, and *d* relaxed states. **b** Force–distance curves obtained by using a hard type cantilever for the A-band regions of single myofibrils in *a* rigor and *b* relaxed states. *Solid lines* represent the first measurement and a *dotted line* the second. The origin of the abscissa is the position of the cantilever at the surface of the cover slip. *Arrows*, the tip of the cantilever just made contact with the surface of the myofibrils. *Asterisk* force versus distance curves for the cover slip

of Fig. 1a. It is known that skinned muscle fibers are radially compressed by the osmotic compression with Dextran, producing uniform spacing changes of the acto-myosin filament lattice [12, 25–27]. Further, the Dextran treatment produces similar changes of the diameter and contractility in isolated single myofibrils [21]. Based on these, the diameter and radial stiffness of the A-band region were examined for single myofibrils immersed in bathing solutions containing various concentrations of Dextran. Typical force–distance curves thus obtained for the A-band regions of rigor and relaxed single myofibrils are shown in Fig. 3. It can be seen that, by increasing the concentration of Dextran, initial rising phases of the force–distance curve are exclusively disappeared, indicating that the A-band regions become shrunken by most elastic components being compressed. Further, the slope of the force–distance curves become increasingly steep, and rigid core-like components get slightly thickdened as the concentration of Dextran is increased, indicating that the A-band region becomes stiffened by the radial compression. These radial changes of the A-band region can be seen as cross-overs of force–distance curves by increasing the Dextran concentration. Consistent with this result, it is reported that the axial and radial stiffness of skinned muscle fiber become stiffened by the radial compression [12]. Force–distance curves obtained for single myofibrils before and after Dextran treatments almost overlap each other (data not shown), suggesting that the A-band regions were reversibly compressed by Dextran. It is reported for skinned muscle fibers that osmotic compressions with Dextran are reversible except at high concentrations of Dextran [26]; i.e., the large diameter of muscle fibers together with high viscosity of Dextran solutions would impede the diffusion of molecules in fiber preparations.

The diameter and the radial stiffness changes of the A-band region depending on the Dextran concentration are summarized in Fig. 4a and b, respectively. The diameter of the A-band region of rigor myofibrils, 0.92 ± 0.01 μm ($n = 5$) with no Dextran was decreased to 0.71 ± 0.02 μm ($n = 5$) by increasing the concentration of Dextran to 2 %, and further decreased to 0.65 ± 0.02 μm ($n = 5$) as the concentration of Dextran was increased to 16 %. The diameter of the A-band region of relaxed myofibrils, 1.01 ± 0.02 μm ($n = 5$) with no Dextran was decreased to

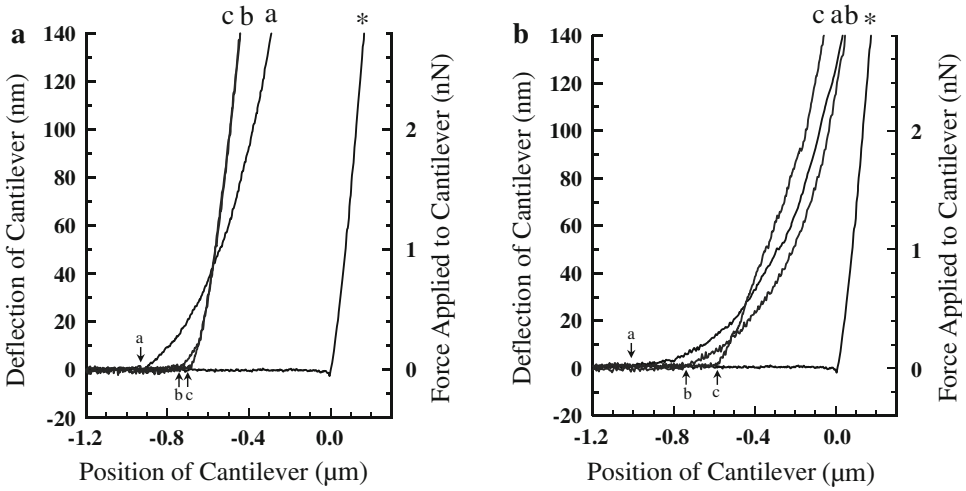

Fig. 3 Force–distance curves for A-band regions of Dextran-treated single myofibrils. **a** Rigor and **b** relaxed myofibrils in *a* 0 %, *b* 2 %, and *c* 8 % Dextran. The origin of the abscissa is the position of the cantilever at the surface of the cover slip. *Arrows* the tip of cantilever just made contact with the surface of the myofibrils. *Asterisk* force versus distance curves for the cover slip

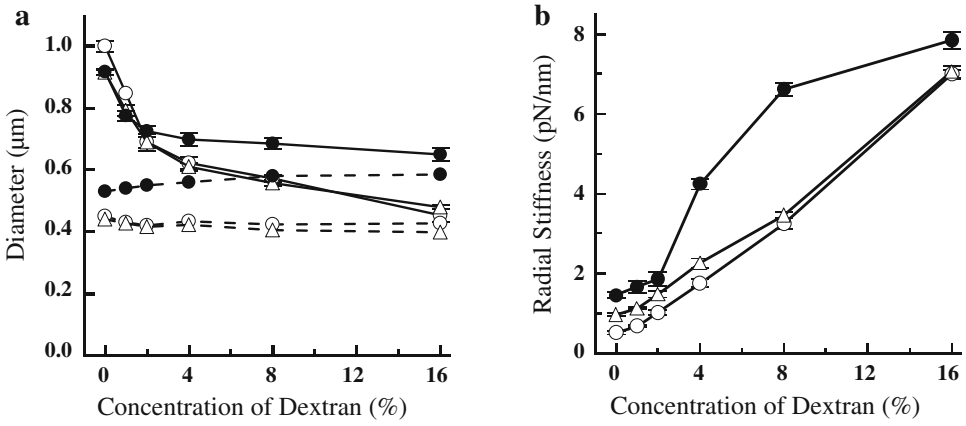

Fig. 4 **a** The diameter and **b** the radial stiffness of the A-band region of Dextran-treated single myofibrils as a function of Dextran concentration. Rigor (*filled circle*), contracting (*opened triangle*) and relaxed (*opened circle*) myofibrils. *Dashed traces* in (**a**) are the thickness of the rigid core. Each data point was normalized by that for myofibrils in the rigor state without Dextran treatment. See text for details

0.68 ± 0.03 μm ($n = 5$) by increasing the concentration of Dextran to 2 %, and gradually decreased to 0.45 ± 0.02 μm ($n = 5$) by further increasing the concentration of Dextran to 16 %. The diameter of the A-band region for contracting myofibrils changed roughly the same as that of relaxed myofibrils by changing the concentration of Dextran. Notably, these Dextran-dependent diameter changes for rigor, contracting, and relaxed myofibrils had clear transitions at about 2 % Dextran. A relatively small effect of the Dextran treatment on the diameter changes of single myofibrils has been reported [21], which could be due to the difference in the experimental conditions. These diameter changes of Dextran-treated single myofibrils are basically in agreement with the spacing changes of the actomyosin filaments lattice in Dextran-treated skinned muscle fibers [27, 28], suggesting that the diameter changes of the A-band region of isolated single myofibrils are directly related to the spacing changes of the actomyosin filament lattice.

The radial stiffness of the A-band region of rigor myofibrils, 1.48 ± 0.07 pN/nm ($n = 5$) with no Dextran, was increased to 1.91 ± 0.17 pN/nm ($n = 5$) as the concentration of Dextran was increased to 2 %, and greatly increased to about 6.60 ± 0.17 pN/nm ($n = 5$) by increasing the Dextran concentration to 8 %, and gradually increased to 7.75 ± 0.21 pN/nm ($n = 5$) by further increasing the Dextran concentration to 16 %. The radial stiffness of relaxed myofibrils, 0.48 ± 0.04 pN/nm ($n = 5$) with no Dextran, was gradually increased to 6.97 ± 0.12 pN/nm ($n = 5$) by increasing the concentration of Dextran up to 16 %. The radial stiffness of contracting myofibrils similarly changed with that of relaxed myofibrils by changing the concentration of Dextran. And, at 16 % Dextran, the radial stiffness of the A-band regions became comparable with rigor, contracting, and relaxed myofibrils.

The thicknesses of the rigid core for Dextran-treated single myofibrils, which were determined from force–distance curves as above, are included in Fig. 4a. It can be seen that, as the concentration of Dextran is increased, the thickness of the rigid cores does not significantly change in the contracting and relaxed states but gets slightly thickened in the rigor state.

The results obtained for Dextran-treated single myofibrils indicate that the A-band region has roughly three stiffness components; i.e., a soft component(s) of 0.5–2.0 pN/nm, a stiff component(s) of 2–8 pN/nm and a rigid core of about 10 pN/nm. The soft component is about 0.2 μm thick for rigor and contracting myofibrils and about 0.3 μm thick for relaxed myofibrils. The stiff component is about 0.3 μm thick for rigor, contracting and relaxed myofibrils and its stiffness significantly greater for rigor myofibrils. The rigid cores detected in the force–distance curves could not clearly be identified in Dextran-treated myofibrils, suggesting that the Dextran treatments could not compress A-band regions up to the rigid cores.

Force–distance curve measurements for the A-band region of single myofibrils in the bathing solution having various ionic strengths

It is known that the lattice spacing of actomyosin filaments in skinned muscle fibers changes depending on the ionic strength [12, 27, 29], suggesting that the electrostatic interaction significantly affects the lattice structure. Based on this, force–distance curves were similarly examined for single myofibrils immersed in bathing solutions having various ionic strengths. Typical force–distance curves of the A-band regions for rigor and relaxed single myofibrils thus obtained are shown in Fig. 5. As the ionic strength was decreased, force–distance curves became increasingly steep and the initial rising phase(s) exclusively disappeared. This can be seen as cross-overs of force–distance curves by decreasing the ionic strength, indicating that the A-band region becomes shrunken and stiff with most elastic components being compressed.

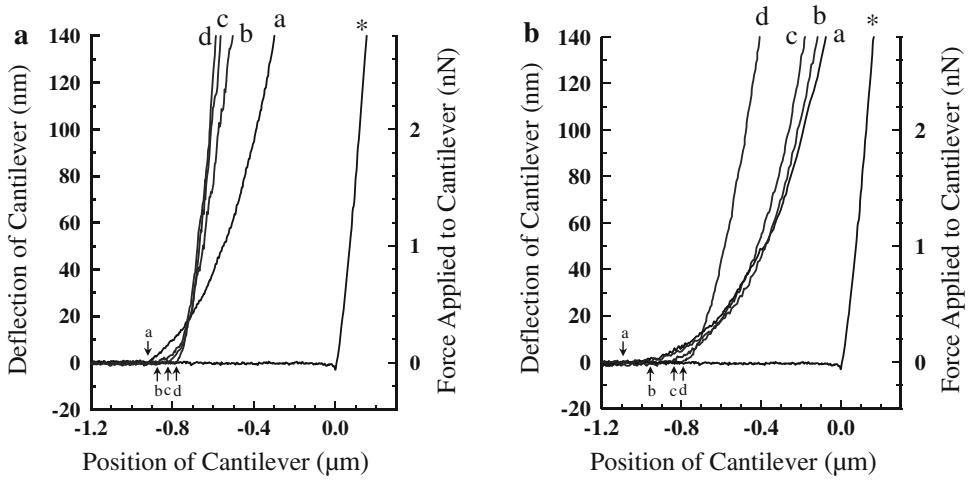

Fig. 5 Force–distance curves for the A-band region of a single myofibril in **a** rigor and **b** relaxing solutions having various ionic strengths. The ionic strength was *a* 200 mM, *b* 140 mM, *c* 80 mM, and *d* 20 mM. The origin of the *abscissa* is the position of the cantilever at the surface of the cover slip. *Arrows* the tip of cantilever just made contact with the surface of myofibrils. *Asterisk* force versus distance curves for the cover slip

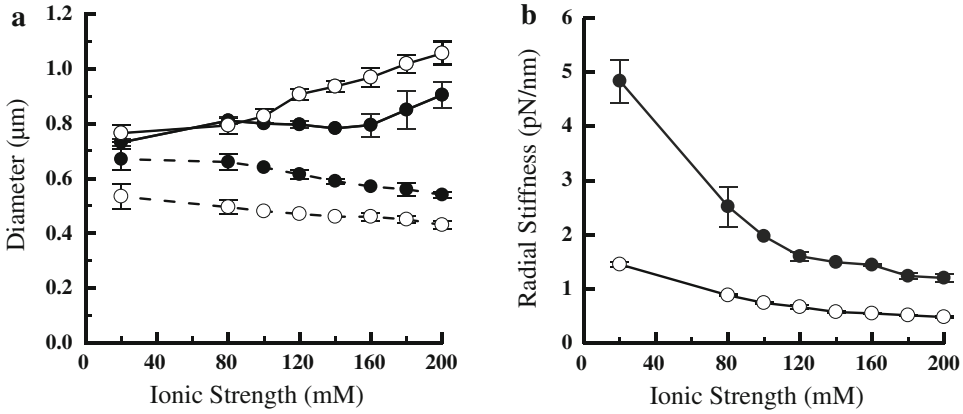

Fig. 6 **a** The diameter and **b** the radial stiffness changes of the A-band regions of single myofibrils depending on the ionic strength of the bathing solution. Rigor (*filled circle*) and relaxed (*opened circle*) myofibrils. *Dashed traces* in (**a**) are the thickness of the rigid core. Each data point was normalized by that for myofibrils in the rigor state at the ionic strength of 200 mM. See text for details

The diameter and the radial stiffness changes of the A-band region depending on the ionic strength are summarized in Fig. 6a and b, respectively. The diameter of rigor single myofibrils was decreased from 0.91 ± 0.05 μm ($n = 5$) to 0.73 ± 0.01 μm ($n = 5$) by decreasing the ionic strength from 200 to 160 mM, and then remained almost unchanged by further decreasing the ionic strength to 20 mM. The diameter of relaxed myofibrils was decreased from 1.05 ± 0.04 μm ($n = 5$) to 0.80 ± 0.03 μm ($n = 5$) by decreasing the ionic strength from 200 to 100 mM, and then stayed almost unchanged by further decreasing the ionic strength to 20 mM. Thus, the diameter of the A-band region decreased by decreasing the ionic strength ($p < 0.01$), which took place in a slightly different ionic strength range between rigor and relaxed myofibrils. And, at an ionic strength below 100 mM, the diameter of A-band regions for rigor and relaxed single myofibrils became almost comparable. These diameter changes of single myofibrils induced by the ionic strength are basically consistent with comparable changes of the lattice spacing changes of skinned muscle fibers [12, 27, 29], again suggesting that the diameter changes of the A-band region of isolated single myofibrils are directly related with the spacing changes of the actomyosin filament lattice.

The thickness of the rigid core was also changed by changing the ionic strength of the bathing solution, the results of which are included in Fig. 6a. As the ionic strength was decreased from 200 to 20 mM, the thickness of rigid core for rigor myofibrils was gradually increased from 0.53 ± 0.05 μm ($n = 5$) to 0.67 ± 0.04 μm ($n = 5$) ($p < 0.05$), and that for relaxed myofibrils slightly but significantly increased from 0.43 ± 0.01 μm ($n = 5$) to 0.53 ± 0.05 μm ($n = 5$) ($p < 0.05$). The radial stiffness of the rigid cores for rigor and relaxed myofibrils was about 10 pN/nm ($n = 5$). Notably, the thickness of the rigid core and the diameter of the A-band region changed in an opposite direction by changing the ionic strength. These results suggest the presence of a component(s) which significantly changes the radial structure depending on the ionic strength, opposite to the direction of the thickness change of the rigid core.

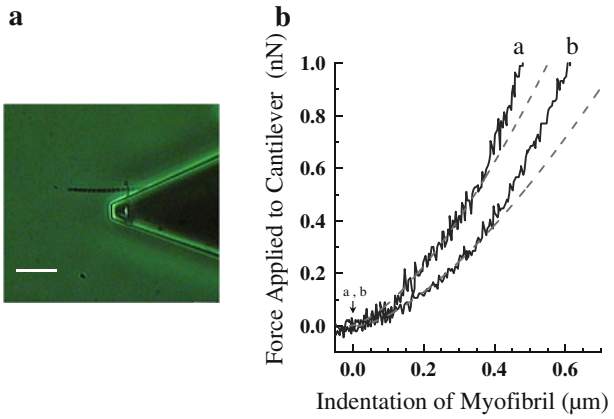

Fig. 7 **a** An optical microscopic image of a rod-tip cantilever positioned over a single myofibril adsorbed onto a cover slip in a criss-cross fashion (*bar* 20 μm). **b** Radial stiffness analysis of the A-band region of single myofibrils. Force–indentation traces are for myofibrils in *a* rigor and *b* relaxed states, and *dashed lines* the best-fit curves to the Hertz equation

The radial stiffness of the A-band region of rigor myofibrils was increased from 1.20 ± 0.08 pN/nm ($n = 5$) to 1.50 ± 0.08 pN/nm ($n = 5$) by decreasing the ionic strength from 200 to 120 mM, and then greatly increased to 4.83 ± 0.40 pN/nm ($n = 5$) by further decreasing the ionic strength to 20 mM. On the other hand, the radial stiffness of relaxed myofibrils was slightly and gradually increased from 0.48 ± 0.02 pN/nm ($n = 5$) to 1.45 ± 0.04 pN/nm ($n = 5$) by decreasing the ionic strength from 200 to 20 mM.

Determinations of the axial Young's moduli of single myofibril and the radial Young's moduli of the A-band regions

The radial Young's modulus for the A-band region was determined as detailed in "Materials and methods" based on force–indentation curves which were transformed from the force–distance curves obtained by compressing single

myofibrils with a rod-type cantilever in a criss-cross fashion as shown in Fig. 7a. As can be seen in Fig. 7b, force–indentation curves could satisfactorily be approximated by the Hertz equation up to about 0.2 μm of indentation (about 20 % of the diameter) for rigor and relaxed myofibrils, namely within the compression ranges of the soft component(s) classified above for Dextran-treated myofibrils. The radial Young's modulus for the soft component thus determined was 62.0 ± 9.8 kPa ($n = 25$) for myofibrils in the rigor state, 58.8 ± 10.7 kPa ($n = 13$) in the contracting state, 36.3 ± 4.8 kPa ($n = 20$) in the (+)AMPPNP state, 10.0 ± 0.3 kPa ($n = 25$) in a low ionic strength state (80 mM), and 4.8 ± 1.7 kPa (n = 11) in the relaxed state. These values are consistent with those obtained by previous AFM studies of skeletal myofibrils; 61–84 and 5–12 kPa for rigor and relaxed myofibrils, respectively [14, 30], and also with those obtained by osmotic compressions of skinned muscle fibers in rigor and relaxed states; 17–39 and 15–16 kPa, respectively [27, 31]. The radial Young's moduli for the other components were not determined, as the filament lattice for these components would be very irregular (see below).

Separately, the axial Young's modulus of isolated single myofibrils was determined based on the sinusoidal-length-change stiffness analysis as detailed in "Materials and methods". Typical traces for length changes applied to single myofibrils and for force responses are shown in Fig. 8a. The axial Young's modulus was 12.2 ± 0.7 MPa ($n = 7$) for myofibrils in the rigor state, 8.8 ± 0.4 MPa ($n = 5$) in the contracting state, 6.3 ± 0.5 MPa ($n = 6$) in the (+)AMPPNP state, 1.6 ± 0.3 MPa ($n = 6$) in a low ionic strength state (80 mM), and 0.4 ± 0.1 MPa ($n = 7$) in the relaxed state. These values are comparable in magnitude to those obtained for skinned muscle fiber: 15–30 MPa in a rigor state, and 4–26 MPa in a contracting state [32, 33].

In Fig. 8b are plotted the axial versus radial Young's moduli determined for single myofibrils in various physiological conditions. It can be seen that the two Young's moduli change in a linear fashion ($r = 0.96$), and that the extrapolation of the regression line hits the ordinate near the origin of *x*- and *y*-axes, consistent with the result of our previous AFM study of skeletal myofibrils [30].

Discussion

Radial stiffness components of the actomyosin filament lattice

In the above studies, the diameter and the radial stiffness of the A-band region of isolated single skeletal myofibrils were examined by using AFM technology. The results obtained by Dextran compressions of single myofibrils supplemented by those obtained by the cantilever compressions clarified that the A-band region had roughly three different stiffness components: soft components (0.5–2.0 pN/nm and 0.2–0.3 μm thick), stiff components (2–8 pN/nm and about 0.3 μm thick), and rigid cores (about 10 pN/nm and 0.5–0.6 μm thick). As the sarcomere length was

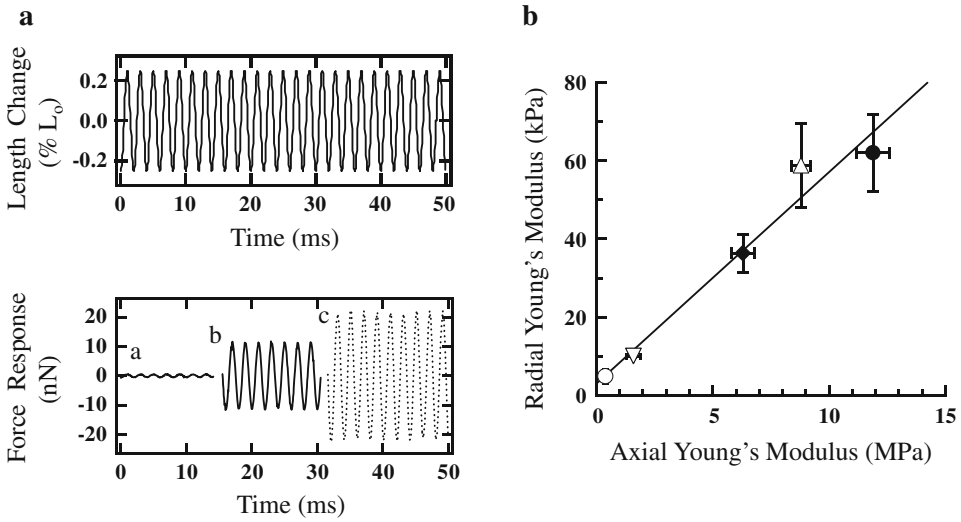

Fig. 8 **a** Axial stiffness analysis of single myofibrils suspended between glass needles. *Upper panel* length changes applied to one end of a preparation, and *lower panel* force responses of the other end of the preparation, in which brief traces are shown for clarity for *a* relaxed, *b* contracting, and *c* rigor states. See details in the text. **b** Relationship between the axial Young's modulus of single myofibrils and the radial Young's modulus of the soft components of the A-band region of single myofibrils in various physiological states. Relaxed (*opened circle*), a low ionic-strength state (80 mM) (*open inverted triangle*), (+)AMPPNP (*filled diamond*), contracting (*opened triangle*), and rigor (*filled circle*)

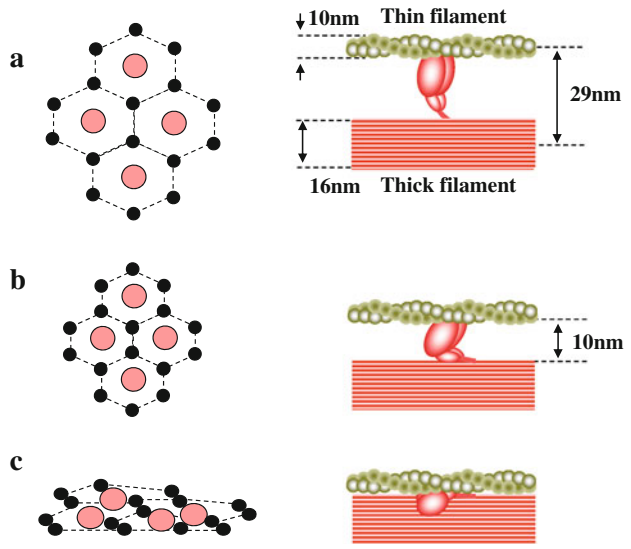

Fig. 9 Schematics of radially compressed actomyosin filament lattice. **a** Intact state, **b** 30 %-compressed state, and **c** 50 %-compressed state. *Left panel* cross-section of the filament lattice, in which *large circles* represent thick filament backbones and *small circles* thin filaments. *Right panel* simplified configurations of cross-bridges, thin filaments, and thick filament backbones shown in the *left panel*

about 2.1 μm for the present myofibril preparations, thin and thick filaments in the A-band regions fully overlapped each other, producing a regular double-hexagonal lattice [2, 18]. Therefore, assuming that the above stiffness components are directly related to the structural elements of the actomyosin filament lattice, we will analyze the results obtained using a simplified lattice model, as depicted in Fig. 9, considering the documented geometry of the filament lattice [2, 34].

Notably, the soft components in rigor, contracting and relaxed myofibrils are all similarly compressed up to about 2 % Dextran (Fig. 4a), suggesting that they come from a common structure(s). As can be seen in Fig. 8b, the radial Young's moduli for the soft components change in a linear fashion with the axial Young's moduli of myofibrils by changing the physiological condition of the myofibrils, and the regression line drawn for the two Young's moduli hits the ordinate near the origin. As the axial stiffness of the muscle fiber increases with the number of myosin heads attached to thin filaments [3], the above results indicate that the soft components almost exclusively come from myosin heads complexed with thin filaments. Notably, the thickness of the soft components, about 30 % of the diameter of the A-band region, is comparable to the range of radial movements of the myosin head relative to the surface of the thick filament backbone via its lever arm. Thus, by radial compression of the soft component, myosin heads extruded from the thick filament backbone may be pushed to thin filaments as shown in Fig. 9b, suggesting that the radial stiffness of the soft component comes from that of the arm region of the myosin filament.

The rigid core of the A-band region is significantly thicker in rigor myofibrils than in relaxed myofibrils. Considering that all myosin heads are attached to and detached from thin filaments in the rigor and relaxed states, respectively [1, 35], the actomyosin filaments lattice would be completely flattened as shown in Fig. 9c in a relaxed state. In a rigor state, a large number of attached myosin heads would forcefully be detached from the thin filaments [36, 37], but a significant number remain attached to thin filaments so that the lattice would not completely be flattened. By taking these differences into consideration, the thickness of the rigid core of A-band may be about 50 % and about 60 % of the diameter in the rigor and relaxed states, respectively, roughly comparable to the thickness of the rigid cores observed. Thus, in the rigid cores, a great number of thin filaments and thick filament backbones would be closely packed with each other, greatly disrupting the regular double-hexagonal lattice structure.

The stiff components have their radial stiffness inbetween the soft components and the rigid cores. Considering the above structural assignments for the soft components and the rigor cores, we may assume that the stiff components come from irregular filament lattices in which the myosin heads are thrust inbetween thin and thick filaments. The stiffness of the stiff components is far greater in a rigor state than in other states, as the myosin heads attached to thin filaments would radially strengthen the lattice structure. In muscle fibers in which the A-band is radially compressed up to the stiff component, the interaction of myosin heads with thin filaments would be significantly hindered, resulting in the suppression of the contractility [4, 5].

Effects of the electrostatic interactions on the radial stability of the actomyosin filament lattice

The present studies showed that the diameter and the radial stiffness of the A-band region in single myofibrils characteristically change depending on the ionic strength of the bathing solution. Namely, the electrostatic force significantly affects the internal structures of the actomyosin filament lattice, in agreement with comparable results for skinned muscle fibers [12, 29]. Notably, the diameter changes of the A-band region produced by the ionic strength are nearly comparable in magnitude to the thickness of the soft components, strongly suggesting that the soft components are sensitive to the electrostatic interactions.

Interestingly, the thickness of the rigid cores for rigor and relaxed myofibrils significantly change, depending on the ionic strength (Fig. 6a), to a direction opposite to the

diameter changes of the A-band region. In the rigid cores, a great number of thin and thick filaments would be closely packed with each other as discussed above, possibly to spacings comparable to the packing space of tobacco mosaic virus molecules. Considering that the thin and the thick filaments are negatively charged [38], we may assume that the thickness increases of the rigid cores produced by decreasing the ionic strength come from the electrostatic repulsive interactions between thin and thick filament backbones, as in the case for tobacco mosaic virus [9]. As far as we know, such distinct electrostatic interactions in the components of the actomyosin filament system observed above have not so far been reported. This may be explained as Dextran treatments of skinned muscle fibers not being able to fully compress A-band regions up to the rigid cores, and as the thickness changes of the rigid core produced by the ionic strength being masked by overall diameter changes of the A-band region.

It is reported that myosin heads make contact with thin filaments in compressed skinned muscle fibers in a relaxed state [39]. Consistent with this, the radial stiffness of relaxed single myofibrils significantly increases with the Dextran treatment at around 2 % Dextran (Fig. 4b), suggesting that the myosin heads are weakly interacting with thin filaments under such a situation. Similarly, at very low ionic strengths, the diameter of the A-band for relaxed myofibrils becomes roughly comparable to that for rigor myofibrils at high ionic strengths while its radial stiffness is small (Fig. 6a, b). This suggests that the myosin heads are very weakly attached to thin filaments in relaxed myofibrils at very low ionic strengths, consistent with the weakly attached state of the myosin heads in relaxed muscle fibers at low ionic strength [40].

Radial stiffness components and the stability of the actomyosin filament lattice

The present studies strongly suggest that the actomyosin filament lattice can be radially compressed greatly and apparently reprimed to the intact configuration when the stresses are removed. Considering that the electrostatic interaction between filamentous molecules is short range [11], the electrostatic repulsive forces between thin filaments and thick filament backbones would become effective only in greatly compressed filament lattices as clarified in the present study. Thus, we may assume that the overall radial stability of the actomyosin filament lattice is primarily maintained via myosin heads inter-connecting thin filaments and thick filament backbones. This is in agreement with the result that the interactions of myosin heads with thin filaments significantly affect the internal structures of actomyosin filaments lattice [41]. Along this line, the interactions of myosin heads with thin filaments and thick filament backbones are directly taken into a recent theoretical analysis for the radial stability of the actomyosin filament lattice [42].

On the other hand, it is known that the lattice spacing of the actomyosin filaments in the overlap region is nearly the same in intact muscle fibers in relaxed, contracting, and rigor states [43]. By skinning relaxed muscle fibers, however, the diameter of the A-band regions gets swollen with uniform spacing increases of the filament lattice [27, 44]. Similarly the present results indicate that the diameter of the A-band region of isolated single myofibrils is significantly thicker in a relaxed state than in a rigor state. These results suggest that a component(s) removed by skinning muscle fibers, e.g., sarcolemma, keeps the actomyosin lattice radially compressed so that the myosin heads are close to the surface of thin filaments in intact muscle fibers.

It can further be noted that the Dextran treatment and the ionic strength change distinctly affect the diameter of single myofibrils and the lattice spacing of the actomyosin filaments of skinned muscle fibers. The Dextran treatment produces significantly greater diameter decreases in single myofibrils (Fig. 4a) compared with the lattice spacing decreases of the actomyosin filaments in skinned muscle fibers [4, 28]. Further, by the ionic strength decrease in a rigor state, the diameter of single myofibrils significantly decreases (Fig. 6a), while the lattice spacing of the actomyosin filaments of single skinned fibers remains almost unchanged [4, 29, 44]. Considering that all myosin heads are attached to thin filaments in a rigor state [35], this suggests that cross-bridges attached to thin filaments have different structures in the two preparations. The above differences can reasonably be explained as some locus in the lever arm region of myosin filaments being radially expanded by the electrostatic repulsive forces in an isolated single myofibril, the movement of which is suppressed in skinned muscle fibers [45, 46].

In the sarcomere of skeletal muscle fiber, thin filaments are anchored to Z-bands and thick filaments bundled together by the M-line and linked to Z-lines via titin filaments [1, 2]. Our previous studies of isolated single myofibrils showed that the radial stiffness of the A-band region is significantly changed by enzymatic digestions of the Z-band and titin [16, 23, 24], suggesting that these components further strengthen the radial structure of the actomyosin filament lattice.

Acknowledgments Technical assistance by A. Hamazaki and Y. Yoshikawa is greatly appreciated. This work was supported in part by Grant-in-Aids for Scientific Research (B) and (C) from the Ministry of Education, Science, Sports, and Culture of Japan (to T.Y.).

Conflict of interest The authors declare that they have no conflict of interest.

References

1. Bagshaw CR (1993) Muscle contraction. Chapman & Hall, London
2. Squire J (1981) The structural basis of muscular contraction. Plenum, New York
3. Gordon AM, Huxley AF, Julian FJ (1966) The variation in isometric tension with sarcomere length in vertebrate muscle fibres. J Physiol 184:170–192
4. Godt RE, Maughan DW (1981) Influence of osmotic compression on calcium activation and tension in skinned muscle fibers of the rabbit. Pflügers Arch 391:334–337
5. Krasner B, Maughan D (1984) The relationship between ATP hydrolysis and active force in compressed and swollen skinned muscle fibers of the rabbit. Pflügers Arch 400:160–165
6. Bernal JD, Fankuchen I (1941) X-ray and crystallographic studies of plant virus preparations. J Gen Physiol 25:111–146
7. Brenner SL, McQuarrie DA (1973) Force balances in systems of cylindrical polyelectrolytes. Biophys J 13:301–331
8. Millman BM, Nickel BG (1980) Electrostatic forces in muscle and cylindrical gel systems. Biophys J 32:49–63
9. Millman BM, Irving TC, Nickel BG, Looseley-Millman ME (1984) Interrod forces in aqueous gels of tobacco mosaic virus. Biophys J 45:551–556
10. Millman BM (1998) The filament lattice of striated muscle. Physiol Rev 78:359–391
11. Matsubara I, Elliott GF (1972) X-ray diffraction studies on skinned single fibres of frog skeletal muscle. J Mol Biol 72:657–689
12. Umazume Y, Onodera S, Higuchi H (1986) Width and lattice spacing in radially compressed frog skinned muscle fibres at various pH values, magnesium ion concentrations and ionic strengths. J Muscle Res Cell Motil 7:251–258
13. Millmann BM, Irving TC (1988) Filament lattice of frog striated muscle: radial forces, lattice stability, and filament compression in the A-band of relaxed and rigor muscle. Biophys J 54:437–447
14. Yoshikawa Y, Yasuike T, Yagi A, Yamada T (1999) Transverse elasticity of myofibrils of rabbit skeletal muscle studied by atomic force microscopy. Biochem Biophys Res Comm 256:13–19
15. Nyland LR, Maughan DW (2000) Morphology and transverse stiffness of Drosophila myofibrils measured by atomic force microscopy. Biophys J 78:1490–1497
16. Akiyama N, Ohnuki Y, Kunioka Y, Saeki Y, Yamada T (2006) Transverse stiffness of myofibrils of skeletal and cardiac muscles studied by atomic force microscopy. J Physiol Sci 56:145–151
17. Friedman AL, Goldman YE (1996) Mechanical characterization of skeletal muscle myofibrils. Biophys J 71:2774–2785
18. Yuri K, Wakayama J, Yamada T (1998) Isometric contractile properties of single myofibrils of rabbit skeletal muscle. J Biochem 124:565–571
19. Tesi C, Colomo F, Nencini S, Piroddi N, Poggesi C (1999) Modulation of substrate concentration of maximal shortening velocity and isometric force in single myofibrils from frog and rabbit fast skeletal muscle. J Physiol 516:847–853
20. Wakayama J, Yamada T (2000) Contractility of single myofibrils of rabbit skeletal muscle studied at various MgATP concentration. Jpn J Physiol 50:533–542
21. Shimamoto Y, Kono F, Suzuki M, Ishiwata S (2007) Nonlinear force-length relationship in the ADP-induced contraction of skeletal myofibrils. Biophys J 93:4330–4341
22. Roark RJ (1965) Formulas for stress and strain. McGraw-Hill, New York
23. Wakayama J, Yoshikawa Y, Yasuike T, Yamada T (2000) Atomic force microscopic evidence for Z-band as a rigid disc fixing the sarcomere structure of skeletal muscle. Cell Struct Funct 25:361–365
24. Kayamori T, Miyake N, Akiyama N, Aimi M, Wakayama J, Kunioka Y, Yamada T (2006) Mechanical strength of sarcomere structures of skeletal myofibrils studied by submicromanipulation. Cell Struct Funct 31:135–143
25. Maughan DW, Godt RE (1981) Radial forces within muscle fibers in rigor. J Gen Physiol 77:49–64
26. Umazume Y, Kasuga N (1984) Radial stiffness of frog skinned muscle fibers in relaxed and rigor conditions. Biophys J 45:783–788
27. Kawai M, Wray JS, Zhao Y (1993) The effect of lattice spacing change on cross-bridge kinetics in chemically skinned rabbit psoas muscle fibers: I. proportionality between the lattice spacing and the fiber width. Biophys J 64:187–196
28. Brenner B, Yu LC (1991) Characterization of radial force and radial stiffness in Ca^{2+}-activated skinned fibres of the rabbit psoas muscle. J Physiol 441:703–718
29. Brenner B, Yu LC, Podolsky RJ (1984) X-ray diffraction evidence for cross-bridge formation in relaxed muscle fibers at various ionic strengths. Biophys J 46:299–306
30. Yamada T, Yoshikawa Y, Wakayama J (1999) Longitudinal and transverse stiffness of single myofibrils of rabbit skeletal muscle in various physiological states. Biophys J 76:A160
31. Maughan DW, Godt RE (1979) Stretch and radial compression studies on relaxed skinned muscle fibers of the frog. Biophys J 28:391–402
32. Kawai M, Brandt PW (1980) Sinusoidal analysis: a high resolution method for correlating biochemical reactions with physiological processes in activated skeletal muscles of rabbit, frog and crayfish. J Muscle Res Cell Motil 1:279–303
33. Tawada K, Kimura M (1984) Stiffness of glycerinated rabbit psoas fibers in the rigor state: filament-overlap relation. Biophys J 45:593–602
34. Brenner B, Xu S, Charovich JM, Yu LC (1996) Radial equilibrium lengths of actomyosin cross-bridges in muscle. Biphys J 71:2751–2758
35. Lovell SJ, Harrington WF (1981) Measurement of the fraction of myosin heads bound to actin in rabbit skeletal myofibrils in rigor. J Mol Biol 149:659–674
36. Nakajima N, Kunioka Y, Nakano K, Shimizu K, Seto M, Ando T (1997) Scanning force microscopy of the interaction events between a single molecule of heavy meromyosin and actin. Biochem Biophys Res Comm 234:178–182
37. Nishizaka T, Seo R, Tadakuma H, Kinosita K, Ishiwata S (2000) Characterization of single actomyosin rigor bonds: load dependence of lifetime and mechanical properties. Biophys J 79:962–974
38. Bartels EM, Elliott GF (1985) Donnan potentials from the A- and I-bands of glycerinated and chemically skinned muscles, relaxed and in rigor. Biophys J 48:61–76
39. Umazume Y, Higuchi H, Takemori S (1991) Myosin heads contact with thin filaments in compressed relaxed skinned fibres of frog skeletal muscle. J Muscle Res Cell Motil 12:466–471
40. Brenner B, Schoenberg M, Chalovich JM, Greene LE, Eisenberg E (1982) Evidence for cross-bridge attachment in relaxed muscle at low ionic strength. Proc Natl Acad Sci USA 79:7288–7291
41. Bershitsky SY, Koubasova NA, Bennett PM, Ferenczi MA, Shestakov DA, Tsatryan AK (2010) Myosin heads contribute to the maintenance of filament order in relaxed rabbit muscle. Biophys J 99:1827–1834
42. Smith DA, Stephenson DG (2011) An electrostatic model with weak actin-myosin attachment resolves problems with the lattice stability of skeletal muscle. Biophys J 100:2688–2697

43. Huxley HE, Brown W (1967) The low-angle x-ray diagram of vertebrate striated muscle and its behaviour during contraction and rigor. J Mol Biol 30:383–434
44. Godt RE, Maughan DW (1977) Swelling of skinned muscle fibers of the frog: experimental observation. Biophys J 19:103–116
45. Huxley HE (1969) The mechanism of muscular contraction. Science 164:1356–1365
46. Burke M, Himmelfarb S, Harrington WF (1973) Studies on the "hinge" region of myosin. Biochemistry 12:701–710